



Effect of annealing on structural and magnetic properties of Pr₂Co₇ compounds

R. Fersi^{a,b}, N. Mliki^a, L. Bessais^{b,*}, R. Guetari^a, V. Russier^c, M. Cabié^d

^a Laboratoire Matériaux Organisation et Propriétés, Faculté des Sciences de Tunis, Université Tunis El Manar, 2092 Tunis, Tunisia

^b CMTR, ICMPE, UMR7182, CNRS – Université Paris Est, 2-8 rue Henri Dunant F-94320, Thiais, France

^c MCMC, ICMPE, UMR7182, CNRS – Université Paris Est, 2-8 rue Henri Dunant F-94320, Thiais, France

^d CP2M, Université Paul Cezanne, F-13397 Marseille, France

ARTICLE INFO

Article history:

Received 13 July 2011

Received in revised form

13 December 2011

Accepted 15 December 2011

Available online 10 January 2012

PACS:

75.50.Bb

75.50.Tt

76.80.+y

Keywords:

Rare-earth intermetallics

Magnetic properties

Mechanical alloying and milling

Diffraction

Magnetic applications

ABSTRACT

Using high-energy ball milling, nanostructured Pr₂Co₇ powders can be obtained from their arc-melted bulk alloys. The structure and the microstructure properties were studied by X-ray diffraction and transmission electron microscopy. The crystallization, phase components and magnetic properties of these alloys were investigated systematically. Structural and magnetic measurements reveal different phases for specific annealing temperature ranges. For samples annealed at $T_a = 1023$ K, the main phase is hexagonal of the Ce₂Ni₇ type structure whereas at $T_a = 1323$ K, the main one is rhombohedral of the Gd₂Co₇ type structure. The autocohereant diffraction domain size derived from Rietveld analysis, varying between 6 and 40 nm, are confirmed by transmission electron microscopy. The coercivity increases with annealing temperature reaching a maximum for $T_a = 1073$ K, the highest value is equal to 18 kOe at 293 K and 23 kOe at 10 K. This coercivity is attributed to the high magnetocrystalline anisotropy of the Pr₂Co₇ phase and its optimized nanoscale grain size. The remanence ratio M_r/M_{max} is equal to 0.64. Thermomagnetic measurements indicate that the intermetallic Curie temperature (T_C) is about 600 K for hexagonal phase and 580 K for rhombohedral one. These properties are suitable for permanent magnet applications.

© 2011 Elsevier B.V. All rights reserved.

1. Introduction

Since last decades, a growing demand from users for magnetic alloys based on rare earth and transition metal for potential applications has emerged. The synthesis of such alloys can lead to powerful magnetic materials characterized by a high Curie temperature and high anisotropy constants [1–4]. Indeed, the combination of high magnetization at room temperature of ferromagnetic transition metals with high magnetic anisotropy is needed to compete with currently marketed SmCo₅ and NdFeB alloys [5,6].

Emphasis is now shifting toward nanoscale world, opening the way to improve microstructure required for permanent magnet and magnetic recording applications. Among the processes able to lead to optimized assemblies, the techniques of melt spinning [7] and high-energy milling, with subsequent annealing [8,9], are suitable to obtain nanocrystalline phases.

In the search for new phases presenting high magnetocrystalline anisotropy, we have investigated the nanocrystalline Pr₂Co₇

intermetallics. They exhibit an excellent magnetic properties as Curie temperature T_C , the magnetocrystalline anisotropy H_A , and an important saturation magnetization M_S [10,11]. In addition, to intrinsic magnetic properties, it is necessary to optimize the extrinsic properties (magnetization remanence and coercive field).

In the present work, the structural characteristics of high-energy ball-milled and subsequently annealed Pr₂Co₇ alloys, *i.e.*, unit-cell parameters and atom positions are reported with Curie temperature measurements. Furthermore, we have optimized the microstructure of those compounds upon appropriate heat treatment in order to obtain a high coercivity.

2. Experiment

Polycrystalline Pr₂Co₇ alloys were prepared by high-energy ball milling. An excess of praseodymium powder was used in order to maintain an overpressure of Pr on the sample. After milling during 5 h, with ball to powder ratio of 15/1 under high purity Ar atmosphere, the powders, wrapped in tantalum foil, were annealed for 30 min in sealed silica tube under 10^{-6} Torr at different temperatures (from 873 K to 1323 K). X-ray diffraction (XRD) patterns were carried out on a Bruker diffractometer with Cu K α radiation. The counting rate was 22 s per scanning step and the step size was 0.04°. An internal Si standard (NBS, SRM 640) was used to measure the unit cell parameters with an accuracy of $\pm 1 \times 10^{-4}$ Å. The XRD data was refined using Rietveld method [12,13] as implemented in the FullProf [14–16] computer code, with the assumption of a peak line profile of Thompson–Cox–Hastings

* Corresponding author.

E-mail address: bessais@glvt-cnrs.fr (L. Bessais).

allowing multiple phase refinement of each of the coexisting phases [15,17,18]. The “goodness-of-fit” indicators R_B and χ^2 are calculated as follows:

$$R_B = \frac{\sum_K |I_K(o) - I_K(c)|}{\sum_K I_K(o)}$$

$I_K(o)$ is the observed Bragg intensity and $I_K(c)$ is the calculated one.

$$\chi^2 = \frac{R_{wp}}{R_{exp}}; R_{exp} = \left[\frac{(N - P + C)}{\sum_K w_K(I_K(o))^2} \right]^{1/2}; R_{wp} = \left[\frac{\sum_K w_K(I_K(o) - I_K(c))^2}{\sum_K w_K(I_K(o))^2} \right]^{1/2}$$

where N is the number of measured points in the diagram, P the number of refined parameters and C the number of constraints.

The full-width-at-half-maximum of the Gaussian H_G and Lorentzian H_L component of the profile function is given by:

$$H_G^2 = u \tan^2 \theta + v \tan \theta + w$$

$$H_L = \zeta \tan \theta + \frac{\xi}{\cos \theta}$$

ξ leads to the auto-coherent domain size by means of the Scherrer formula ($\Phi(\text{nm}) = 180 \times 2\lambda_{\text{Cu}(\text{nm})} / \Pi^2 \zeta$). The u, v, w are the adjustable parameters which characterize the contribution of the diffractometer. The various structural parameters: atomic positions, Debye–Waller factor, occupancy parameter s , cell parameters and the u and ξ profile parameters were least-square fitted.

Microstructure observations were made with a JEOL 2010F transmission electron microscope operating at 200 kV and equipped with a field emission gun.

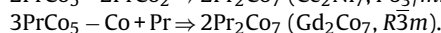
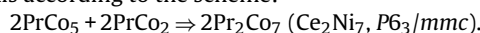
The Curie temperature (T_C) was measured on a differential sample magnetometer MANICS in a field of 1000 Oe with around 5–10 mg sample sealed under vacuum in silica tube in order to prevent oxidation under heating. T_C was determined from the M - T curve by extrapolating the linear part of the M - T curve and finding the temperature value of the intersection with the extended baseline [19,20].

Magnetic hysteresis M - H measurement was performed using a Physical Properties Measurement System (PPMS9) Quantum Design, at $T = 10$ K and 293 K with the field up to 90 kOe.

3. Results and discussion

3.1. Structure analysis

The Pr_2Co_7 compound was found to crystallize in two polymorphic forms. The low temperature phase of the hexagonal Ce_2Ni_7 type structure ($P6_3/mmc$ space group), and the high temperature phase of the rhombohedral Gd_2Co_7 type structure ($R\bar{3}m$ space group) [21]. These phases can be obtained by stacking the hexagonal structural blocks for PrCo_5 (CaCu_5 type structure) and the cubic blocks PrCo_2 (MgCu_2 type structure) along the common hexagonal axis according to the scheme:



The unit cell for the hexagonal structure contains two equivalent crystallographic sites for Pr at 4f and five Co at 12k, 6h, 4f, 4e and 2a. However, the unit cell for the rhombohedral structure contains two equivalent crystallographic sites for Pr at 6c and five Co at 6c, 9e, 3b and 18h (Fig. 1).

Fig. 2 presents, the Rietveld analysis result of XRD pattern of Pr_2Co_7 samples annealed at 1023 K, 1073 K and 1323 K. The result of the structure refinement performed for the sample annealed at 1023 K shows the presence of a main phase with the hexagonal structure. The lattice parameters are $a = 5.068$ Å and $c = 24.463$ Å. This result suggests that the Pr_2Co_7 structure is isotypic with the crystal structure of Ce_2Ni_7 . With increasing the annealing temperature from 1023 K to 1323 K, the rhombohedral phase increases while the hexagonal one decreases. However, we note minor quantities of the oxide phases appearing due to selective oxidation of Pr (PrO , PrO_2 , Pr_2O_3). For the sample annealed at 1323 K, the structure refinement shows the presence of a main phase with the rhombohedral Pr_2Co_7 alloys. The lattice parameters are $a = 5.068$ Å and $c = 36.549$ Å. A comparison with X-ray diffraction diagrams of the Pr_2Co_7 compound showed that Pr_2Co_7 and Gd_2Co_7 are isotypic.

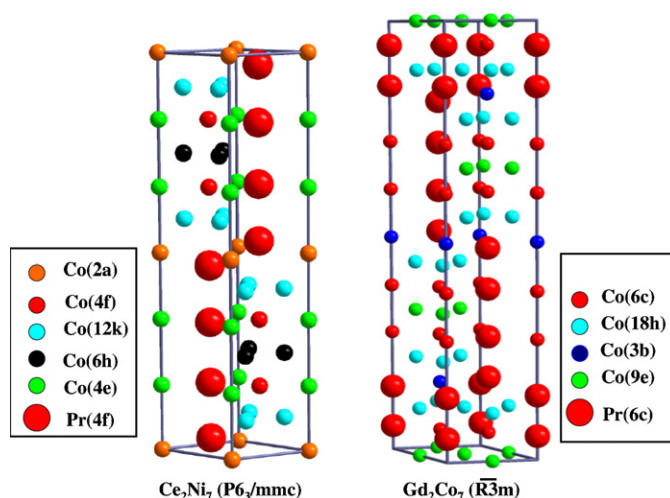


Fig. 1. Crystal structures of Pr_2Co_7 compounds: at left the hexagonal-type structure ($P6_3/mmc$ space group) and at right the rhombohedral-type structure ($R\bar{3}m$ space group).

The lattice parameters, the atomic positions, R_B and χ^2 factors from Rietveld fit are given in Table 1. These values of structural parameters are in agreement with the results obtained previously [22,21]. The auto-coherent diffraction domain size derived from

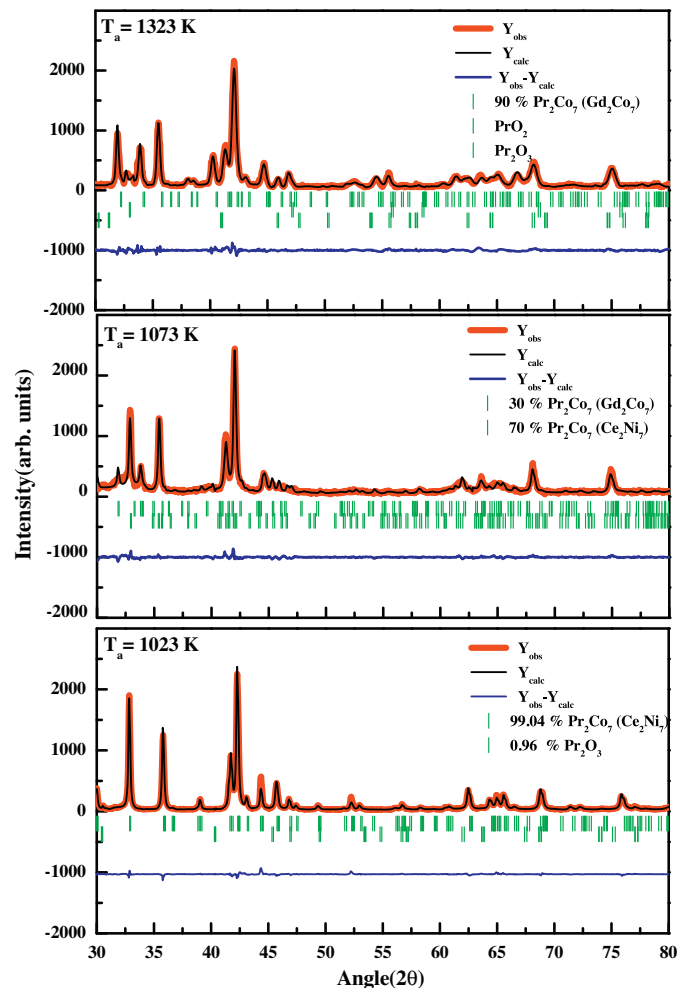


Fig. 2. Rietveld analysis for X-ray diffraction patterns of Pr_2Co_7 compounds annealed at 1023 K, 1073 K and 1323 K for 30 min.

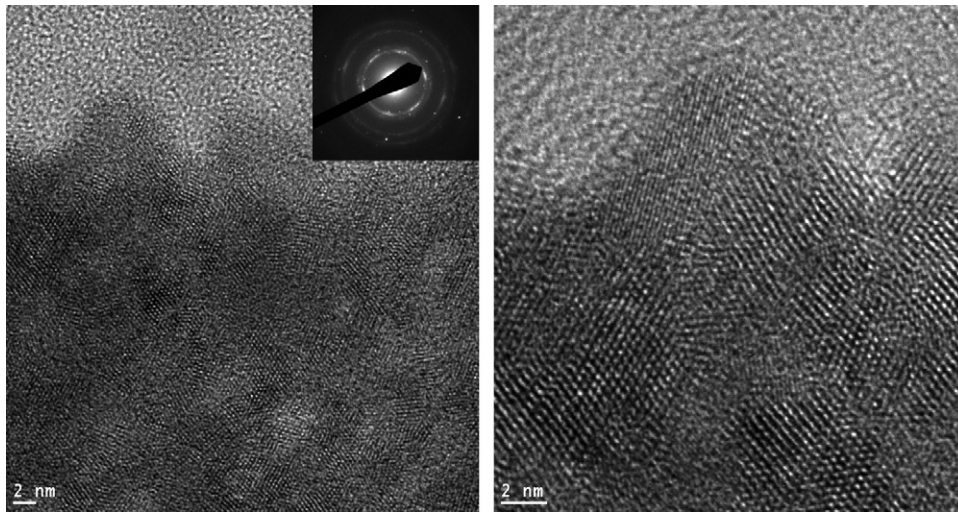


Fig. 3. HRTEM images showing the nanocrystalline aspect of Pr_2Co_7 , inset: corresponding selected area electron diffraction.

Rietveld analysis is $\Phi=6\text{ nm}$ at 1023 K and $\Phi=40\text{ nm}$ at 1323 K these results are corroborated with high resolution transmission electron microscopy (HRTEM).

Fig. 3 shows HRTEM micrographies of the Pr_2Co_7 compound corresponding to the sample annealed at 1073 K. The average grain size is about 6 nm. This result agrees well with the average grain size found by using the Scherrer's formula (Rietveld analysis). In inset we show a selected area electron diffraction of the Pr_2Co_7 compound. One can see a system of concentric rings confirming the polycrystalline aspect of samples: distribution of fine grains disoriented relatively to each other.

3.2. Intrinsic magnetic properties

The Curie temperature, also called the magnetic ordering temperature is a direct measure of the exchange interaction, which is the origin of ferromagnetism. This interaction depends markedly on the interatomic distance. Generally, the Curie temperature in rare-earth transition-metal intermetallic compounds is governed by three kinds of exchange interactions, namely, the $3d-3d$ exchange interaction ($J_{\text{Co-Co}}$) between the magnetic moments of the Co sublattice, $4f-4f$ exchange interaction ($J_{\text{Pr-Pr}}$) between the magnetic moments within the Pr sublattice, and the intersublattice $3d-4f$ exchange interaction ($J_{\text{Pr-Co}}$) [23]. The interactions between the rare earth spins $4f-4f$ are assumed to be weak and negligible in

comparison with the other two types of interactions [24]. The thermal variation of magnetization is plotted in Fig. 4 for the two samples.

This indicates that Pr_2Co_7 phases are ferromagnetic with Curie temperature of 600 K for the hexagonal phase and 580 K for rhombohedral one. This high Curie temperature in Pr_2Co_7 compounds is due to the predominance of the interactions Co–Co.

The magnetization curves $M-H$ obtained at 293 K is represented in Fig. 5 for Pr_2Co_7 . It shows that at 293 K the saturation is not reached, which gives evidence for a magnetocrystalline anisotropy among the highest known in those kinds of systems. The saturation magnetization M_S was deduced using the saturation approach law $M(H)=M_S+a/H^2$. The saturation magnetization is found equal to 67 emu/g, corresponding to $8.32\ \mu_B/\text{u.f.}$ The remanent magnetization M_r is equal to 42.7 emu/g, which gives a remanence ratio $M_r/M_{\text{max}}=0.64$. $M_r/M_{\text{max}} > 0.50$, which suggests magnetic exchange interactions between adjacent crystallites in these nanostructured powders [25,26].

The diffraction pattern obtained for a sample of Pr_2Co_7 oriented magnetic field at room temperature shows that anisotropy enhances the diffraction peaks of type $(00l)$. This allows us to conclude that the easy magnetization is along the c -axis (Fig. 6). The indexation of peaks was made by comparison with the spectrum of Pr_2Co_7 compound without applying magnetic field.

Table 1
 a and c cell parameters, grain size Φ , R_B and χ^2 factors from Rietveld fit for Pr_2Co_7 .

T_a	1023 K	T_a	1323 K
Space group	$P6_3/mmc$	Space group	$R\bar{3}m$
a (Å)	5.068(3)	a (Å)	5.068(4)
c (Å)	24.463(2)	c (Å)	36.549(6)
c/a	4.826	c/a	7.211
$V(\text{Å}^3)$	528.63	$V(\text{Å}^3)$	813.16
χ^2	3.82	χ^2	3.74
R_B	3.72	R_B	6.95
$x\{12k\}\text{Co}$	0.166	$z\{18h\}\text{Co}$	0.111
$y\{12k\}\text{Co}$	0.332	$z\{6c\}\text{Pr}$	0.055
$z\{12k\}\text{Co}$	0.085	$z\{6c\}\text{Pr}$	0.149
$x\{6h\}\text{Co}$	0.164	$z\{6c\}\text{Co}$	0.280
$y\{4f\}\text{Pr}$	0.329	$z\{6c\}\text{Co}$	0.377
$z\{4f\}\text{Pr}$	0.517	–	–
$z\{4f\}\text{Pr}$	0.672	–	–
$z\{4e\}\text{Co}$	0.167	–	–
Φ (nm)	6	Φ (nm)	40
T_C (K)	600	T_C	580

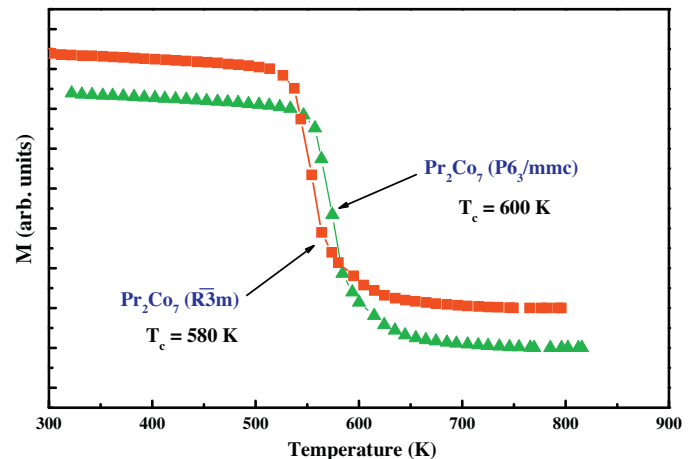


Fig. 4. Thermomagnetization curves of Pr_2Co_7 compounds.

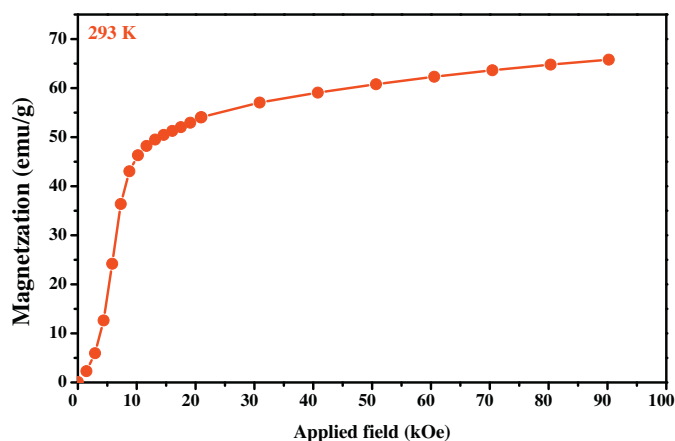


Fig. 5. Magnetization curves of Pr_2Co_7 obtained after high-energy milling and annealed at 1073 K for 30 min, measured at 293 K.

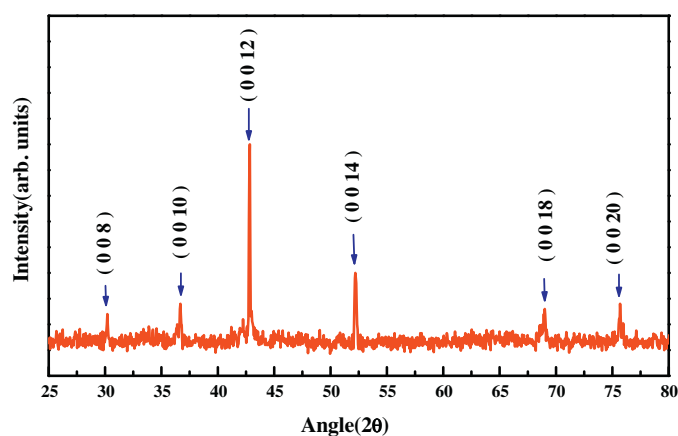


Fig. 6. XRD patterns of oriented powder of Pr_2Co_7 .

3.3. Extrinsic magnetic properties

In order to study the extrinsic properties, we have optimized the Pr_2Co_7 microstructure, which can lead us to the best coercivity. We have therefore used, for this compound, several annealing at different temperatures.

Fig. 7 shows the hysteresis loop at 293 K, as an example, for the sample annealed at 1073 K.

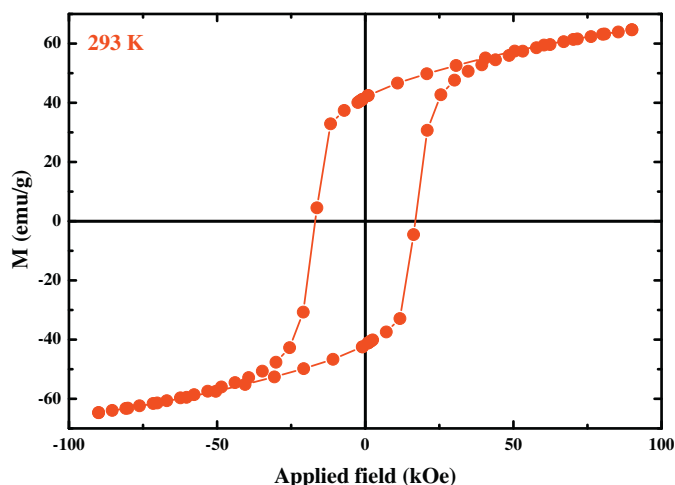


Fig. 7. Hysteresis loop of Pr_2Co_7 annealing at 1073 K for 30 min, measured at 293 K.

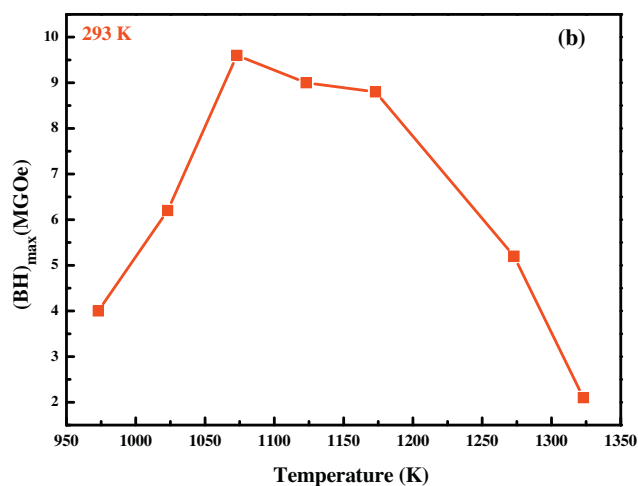
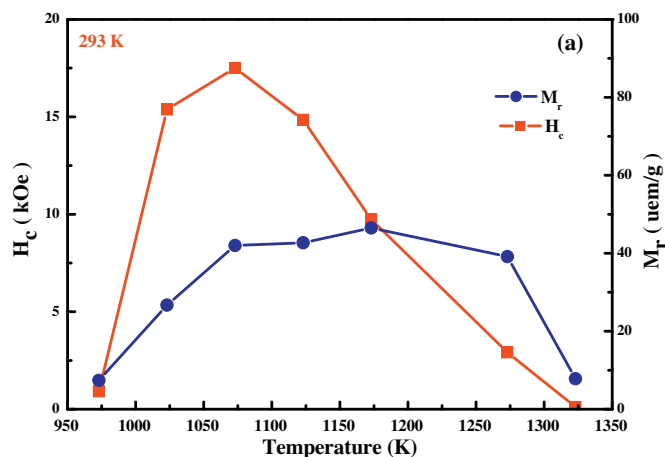


Fig. 8. Magnetic properties: H_c , M_r (a) and $(BH)_{\max}$ (b) as a function of annealing temperature in Pr_2Co_7 .

Fig. 8(a) shows the evolution of the coercivity and the remanent magnetization as a function of annealing temperature. The effect of annealing temperature (T_a) on coercivity is well demonstrated. The coercivity increases with increasing annealing temperature up to 18 kOe ($T_a = 1073$ K). The small coercivity for an annealing temperature of 973 K might be due to an unfavorable microstructure; probably due to the small grain size and many defaults. Furthermore, it is well established that the coercivity decreases with increasing grain size *i.e.* with increasing annealing temperature, which is the reason of the small H_c value for $T_a = 1323$ K. Moreover, for the annealing temperature $T_a = 1073$ K, we have obtained $H_c = 18$ kOe, $M_r = 42.2$ emu/g and $(BH)_{\max} = 9.6$ MGOe (Fig. 8(b)) measured at room temperature, and $H_c = 23$ kOe, $M_r = 50$ emu/g and $(BH)_{\max} = 17.6$ MGOe at $T = 10$ K.

The high magnetic properties observed in these nanostructured Pr_2Co_7 intermetallic alloys might have their origin in their relatively high uniaxial magnetocrystalline anisotropy field and in the homogeneous nanostructure developed by mechanical milling process and subsequent annealing.

4. Conclusion

The Pr_2Co_7 intermetallic compounds crystallize in two polymorphic forms a hexagonal phase of the Ce_2Ni_7 type structure and a rhombohedral one of the Gd_2Co_7 type structure. Highly anisotropic uniaxial ferromagnet is obtained with the easy magnetization

direction parallel to the *c*-axis. No saturation reached at room temperature for applied field of 90 kOe.

Thermomagnetic measurements of Pr₂Co₇ intermetallic show a Curie temperature (*T*_C) about 600 K for Pr₂Co₇ hexagonal phase and 580 K for the rhombohedral one. Furthermore, we show that Pr₂Co₇ exhibits a high coercivity of about 18 kOe at room temperature and 23 kOe at 10 K. The best (*BH*)_{max} value is obtained on samples annealed at a temperature ranged between 1073 K and 1173 K. These interesting intrinsic and extrinsic properties of Pr₂Co₇ are suitable for permanent magnet applications.

References

- [1] A. Margarian, H.S. Li, J.B. Dunlop, J.M. Cadogan, J. Alloys Compd. 239 (1996) 27.
- [2] H. Pan, Y. Chen, X. Han, C. Chen, F. Yang, J. Magn. Magn. Mater. 185 (1998) 77.
- [3] C. Djega-Mariadassou, L. Bessais, A. Nandra, E. Burzo, Phys. Rev. B 68 (2003) 24406.
- [4] L. Bessais, C. Djega-Mariadassou, A. Nandra, M.D. Appay, E. Burzo, Phys. Rev. B 69 (2004) 64402.
- [5] L. Cataldo, A. Lefevre, M. Cohen-Adad, H. Grard, J. Chim. Phys. A 94 (1997) 1087.
- [6] R. Street, R.K. Day, J. Dunlop, J. Magn. Magn. Mater. 69 (1987) 106.
- [7] O. Gutfleisch, N.M. Dempsey, A. Yan, K.H. Müller, D. Givord, J. Magn. Magn. Mater 272 (2004) 647.
- [8] P.G. McCormick, J. Ding, E.H. Feuttrill, R. Street, J. Magn. Magn. Mater 157 (1996) 7.
- [9] L. Bessais, C. Djega-Mariadassou, H. Lassri, N. Mliki, J. Appl. Phys. 106 (2009) 103904.
- [10] K.H.J. Buschow, J. Less-Common Met. 33 (1973) 311.
- [11] H. Kirchmayr, C. Pollidy, J. Magn. Magn. Mater. 8 (1978) 1.
- [12] H. Rietveld, Acta Crystallogr. 22 (1967) 151.
- [13] H. Rietveld, J. Appl. Crystallogr. 2 (1969) 65.
- [14] J. Rodríguez-Carvajal, Physica B 192 (1993) 55.
- [15] J. Rodríguez-Carvajal, M.T. Fernandez-Diaz, J.L. Martinez, J. Phys. 81 (2000) 210.
- [16] L. Bessais, K. Younsi, S. Khazzan, N. Mliki, Intermetallics 19 (2011) 997.
- [17] L. Bessais, S. Sab, C. Djega-Mariadassou, N.H. Dan, N.X. Phuc, Phys. Rev. B 70 (2004) 134401.
- [18] L. Bessais, E. Dorolti, C. Djega-Mariadassou, J. Appl. Phys. 97 (2005) 013902.
- [19] S. Khazzan, N. Mliki, L. Bessais, J. Appl. Phys. 105 (2009) 103904.
- [20] L. Bessais, C. Djega-Mariadassou, Phys. Rev. B 63 (2001) 054412.
- [21] Y. Khan, Acta Crystallogr. 30 (1974) 1533.
- [22] K.J. Strnat, A.E. Ray, H.F. Mildrum, IEEE Trans. Magn. 13 (1977) 1323.
- [23] K.H.J. Buschow, Rep. Prog. Phys. 40 (1977) 1179.
- [24] D. Givord, R. Lemaire, IEEE Trans. Magn. 10 (1974) 109.
- [25] R. Fischer, H. Kronmuller, Phys. Rev. B 54 (1996) 7284.
- [26] R. Fischer, H. Kronmuller, J. Magn. Magn. Mater. 191 (1999) 225.